

PAKISTAN JOURNAL  
OF  
SCIENTIFIC AND INDUSTRIAL RESEARCH

Vol. 6, No. 3

July 1963

**JUMPS IN ACTIVATION ENERGY OF FLOW AND DISCRETE CLUSTER FORMATION IN MOLTEN METALS WITHIN 150°C. OF THE FREEZING POINT**

MAZHAR M. QURASHI

*Physics Division, Central Laboratories, Pakistan Council of Scientific and Industrial Research, Karachi*

(Received March 27, 1963)

The anomalous behaviour of four molten high-purity metals is re-examined in the light of the occurrence of sharp jumps in the activation energy for flow of several simple liquids like water and ethylene glycol. Using the measurements of Yao and Kondic on tin, zinc, aluminium and lead, the activation energies are calculated at small intervals with the equation

$$E_{\eta}/R = + \Delta \ln \eta / \Delta (1/T) = - T^2 \Delta \ln \eta / \Delta T$$

The graphs for  $E_{\eta}/R$  against temperature show several regions of nearly constant  $E_{\eta}$  with sharp drops between them, which agree with Jones and Bartlett's work on aluminium, and can be interpreted as changes in volume of the aggregates or 'clusters', whence the presence of a succession of discrete clusters is deduced. The clusters give reasonable coordination numbers, those formed within 5°C. of the freezing point having linear dimensions of 0.2 micron or more, which compare well with those of the 'mosaic' blocks in actual crystals.

### 1. Introduction

In an earlier communication,<sup>1</sup> it was shown from the available viscosity data of Yao and Kondic<sup>2</sup> and Jones and Bartlett,<sup>3</sup> on high purity molten tin, zinc and aluminium that each of the  $\ln \eta$  versus  $1/T$  plots are best fitted by three consecutive linear segments of markedly different slopes, rather than by a continuous smooth curve as previously believed.<sup>4</sup> From the values of the slopes  $\Delta \ln \eta / \Delta (1/T)$  of these segments, some estimates of the activation energies  $E_{\eta}$  for viscous flow were made, and a large jump (of the order of ten to twenty times the latent heat of fusion) was noted in each of the three metals a few degrees above the melting point. It is the purpose of the present paper to analyse these and other viscosity data more fully and to suggest a possible explanation that may provide some insight into the physical basis of these anomalies.

For the present analysis, use has been made of the differential technique employed in the interpretation of the earlier data on water by Qurashi and Ahsanullah,<sup>5</sup> and found so successful in the experiments carried out on the accurate measurement of  $E_{\eta}$  for a series of pure liquids and solutions in this laboratory (Qurashi et al.),<sup>6-9</sup> cf. (Fig. 1). The basis is of course to evaluate  $E_{\eta}$  from the equation

$$E_{\eta}/R = \Delta \ln \eta / \Delta (1/T) = - T^2 \Delta \ln \eta / \Delta T \quad (1)$$

which is the analytical equivalent of taking the slope of the  $\ln \eta$  versus  $1/T$  graph in the small range  $T, T + \Delta T$ . In this way, the full accuracy of the experimental data is automatically utilized, and a more definite picture of the temperature variation of  $E_{\eta}$  can be obtained.

### 2. Temperature Variation of $E_{\eta}/R$ for Four High-purity Metals

Although the experimental data of Yao and Kondic,<sup>2</sup> used in these calculations, has a relatively high degree of reproducibility with a root-mean-square deviation of  $\pm 0.025$  centipoise i.e.  $\sim 1\%$  for tin,  $\pm 0.08$  c.p. i.e.  $2\%$  for zinc and  $\pm 0.05$  c.p. i.e.  $1.5\%$  for aluminium, nevertheless these data on molten metals are necessarily less accurate than those obtainable on water and aqueous solutions. Therefore, to reduce the effect of random errors on the accuracy of  $E/R$ , the values of viscosity at successive temperatures were first averaged and  $E_{\eta}/R$  was then calculated with equation (1), taking the 'measuring' interval,  $\Delta T$ , as between successive averaged readings. The standard deviations for  $E/R$  were estimated from those of  $\eta$  (and also  $\Delta T$  when less than 2°C.).

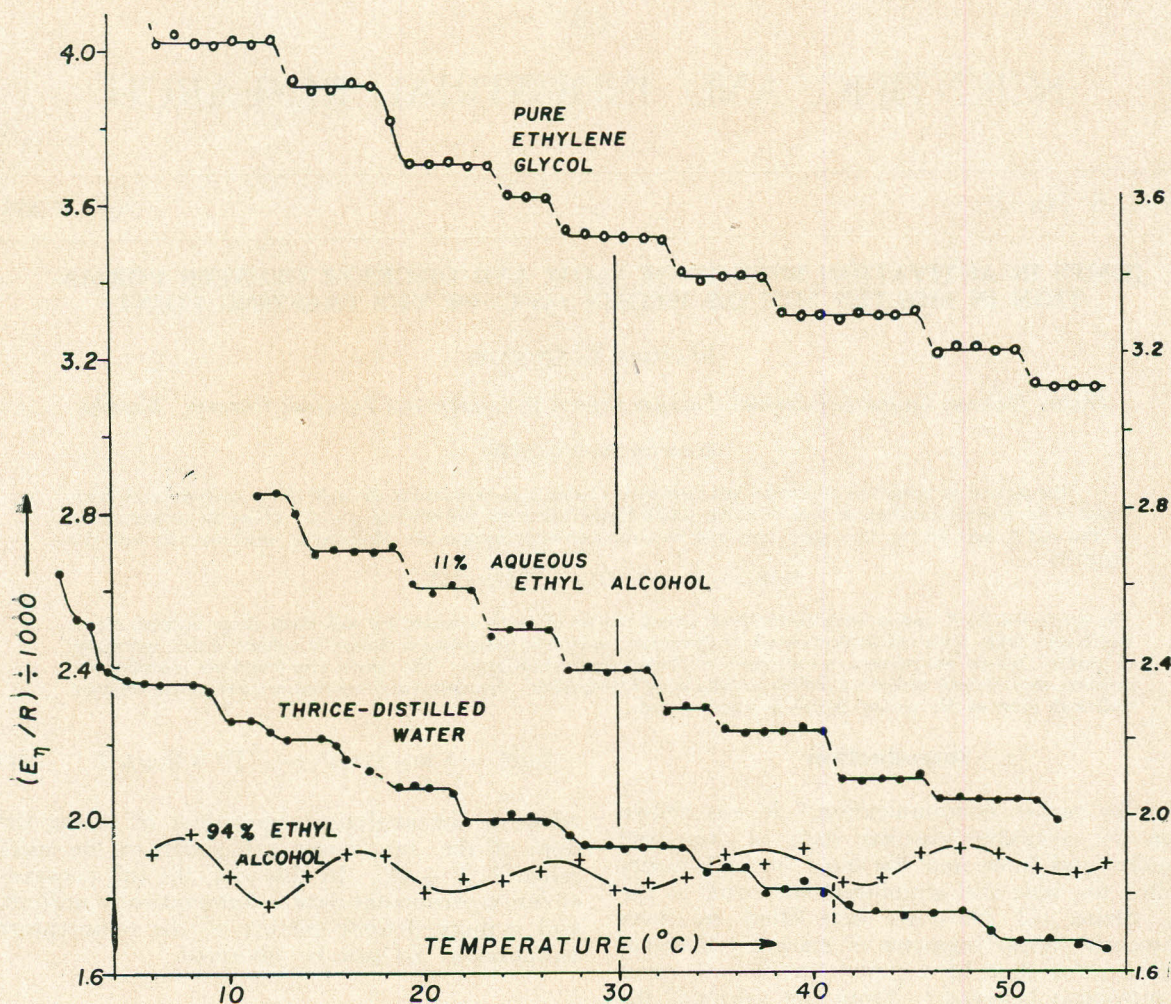


Fig. 1.—Graphs showing the steps (and undulating segments) in the published experimental values of  $E_{\eta}/R$  at close intervals for (i) ethylene glycol, hollow circles, (ii) thrice-distilled water, lower solid circles, (iii) 11% aqueous ethyl alcohol, upper solid circles, and (iv) 94% ethyl alcohol, crosses. The data on water above 41°C. were obtained with  $\Delta T = 1.5^{\circ}\text{C}$ .

In carrying out the calculations for tin as shown in Table 1, the two relatively close readings at 281° and 285°C. have been replaced by a weighted mean at 282.3°C. The calculated values of  $E_{\eta}/R$  are plotted against the mean temperatures in Fig. 2 (a), with the short vertical lines indicating the estimated standard deviations, and a mean graph is drawn through the points, the broken line being the high-temperature value used by McLaughlin and Ubbelohde.<sup>4</sup> Taking  $R = 2$  cal./mole, this graph shows that  $E_{\eta}$  is nearly constant at  $25 \pm 5$  kcal./mole ( $P_1$  in Fig. 2(a)) from 231°C. to 236°C., and then drops sharply to a value of  $3.5 \pm 0.5$  kcal./mole ( $Q_1$  in Fig. 2(a)) for the range of 240°C. to 270°C. before approaching the

mean high-temperature value of 1.1 kcal./mole. Altogether, 90% of the drop from the maximum of 25 kcal. to the intermediate value of 3.5 occurs in less than 3°C. from 236° to 239°C., thus providing strong confirmatory evidence for the existence of these two definite energy values. After 270°C., the  $E_{\eta}/R$  curve again drops sharply, and the plotted points lie around the mean high-temperature value (broken line), but are best fitted by the undulating full-line curve. Although these undulations are of the order of the large standard deviations of the plotted points in this region (being almost as large as the values of  $E_{\eta}/R$ ), it is noteworthy that a sinusoidal variation has previously been observed in 94% ethyl alcohol<sup>9</sup> (Fig. 1.)

Similar calculations were next made for crown zinc and super-pure aluminium, but as the available data<sup>2</sup> for these higher melting metals is less closely spaced than for tin, it is now advantageous to take means of successive readings only above 444 °C. for zinc, the remaining calculations for  $E_\eta/R$  being then carried out with equation 1. These calculated values for zinc and aluminium are plotted in Fig. 2(b), the temperature scale for aluminium (hollow circles) having been shifted 200°C. to the left. After

making allowance for the gap of about 11°C. in the data for zinc, it appears fairly certain that both these metals show two distinct energy values, marked  $P_2, Q_2$  and  $P_3, Q_3$ , above the high-temperature limit, although the extent of the region at P is not as certain as for tin, because of the relatively poor data. There is a sharp drop from the value at P to the intermediate value Q, and a somewhat less steep drop from Q to the lowest (cf. ref. 1). Finally, the inset to Fig. 2(b) shows a similar plot of the fragmentary

TABLE I.—MEAN EXPERIMENTAL VALUES FOR THE VISCOSITY OF MOLTEN TIN, (THE DEVIATIONS BEING GIVEN FOR THE 2ND DECIMAL PLACE) TOGETHER WITH THE VALUES OF  $E_\eta/R$  CALCULATED AT SHORT INTERVALS; THE LAST COLUMN GIVES  $\ln(1/A)$  AS CALCULATED FROM EQUATION (4).

Temp. (°C.)	Observed $\eta$ (centipoises)	Averaged $\eta$ for successive temp. (centipoise)	$E_\eta/R$ 1000	Mean temp. (°C.)	$E_\eta/RT$	$\ln(1/A)$
231	2.71±4					
232	2.65 <sub>5</sub> ±2 <sub>5</sub>	2.68 <sub>2</sub>	10±2	231.9	20.4	24±4
232.5	2.55±1	2.60 <sub>2</sub>	21±4	232.5	} 28.2	32±6
233	2.45±1	2.50 <sub>0</sub>	8±2	233.4		
235	2.36 <sub>5</sub> ±1 <sub>5</sub>	2.40 <sub>8</sub>	10±2	234.6	19.1	23±4
235.5	2.23±3	2.29 <sub>8</sub>	15±3	235.6	30.0	34±6
236.5	2.16 <sub>5</sub> ±5 <sub>5</sub>	2.19 <sub>8</sub>	2.4±0.5	238.4	4.7	8.5±1.0
245	2.04 <sub>5</sub> ±5 <sub>5</sub>	2.10 <sub>5</sub>	1.6±0.3	245.2	3.0	6.9±0.6
254	1.95 <sub>5</sub> ±1 <sub>5</sub>	2.00 <sub>0</sub>	1.5±0.3	252.8	2.8	6.8±0.6
258	1.90 <sub>5</sub> ±1 <sub>5</sub>	1.93 <sub>0</sub>	2.1±0.6	257.8	4.0	7.9±1.1
261	1.85 <sub>5</sub> ±3 <sub>5</sub>	1.88 <sub>0</sub>	1.3±0.4	262.2	2.5	6.4±0.8
269	1.81±5	1.83 <sub>2</sub>	1.2±0.2	270.3	2.2	6.2±0.4
282.3	1.70±3 <sub>5</sub>	1.75 <sub>5</sub>	1.0±0.2	281.6	1.9	5.9±0.4
293	1.67±3	1.68 <sub>5</sub>	0.3±0.3	291.7	0.5	4.6±0.5
298.5	1.67 <sub>5</sub> ±2 <sub>5</sub>	1.67 <sub>2</sub>	0.3±0.3	300.5	0.4	4.5±0.5
312	1.64 <sub>5</sub> ±4 <sub>5</sub>	1.66 <sub>0</sub>	0.5±0.2	312.1	0.9	5.0±0.4
326	1.60 <sub>5</sub> ±2 <sub>5</sub>	1.62 <sub>5</sub>	0.6±0.2	324.5	1.0	5.1±0.4
334	1.58 <sub>5</sub> ±2 <sub>5</sub>	1.59 <sub>5</sub>	1.1±0.3	334.8	1.8	5.9±0.5
345	1.52±1	1.55 <sub>2</sub>	0.9±0.3	343.2	1.4	5.6±0.5
349	1.53±1	1.52 <sub>5</sub>	0.5±0.3	349.5	0.8	5.0±0.5
355	1.51±2	1.52 <sub>0</sub>	0.6±0.3	356.1	} 0.6	4.8±0.3
365.5	1.49±1	1.50 <sub>0</sub>	0.2±0.3	365.4		
375.5	1.50 <sub>5</sub> ±0 <sub>5</sub>	1.49 <sub>8</sub>	-0.1±0.3	375.2	} 0.1	4.3±0.3
384	1.50±2	1.50 <sub>2</sub>	+0.2±0.3	382.6		
387	1.49±3	1.49 <sub>5</sub>				
	Random error < 0.026					

data<sup>2</sup> for super-pure lead, which again gives some evidence of the two steps corresponding to P and Q.

### 3. Possible Interpretation in Terms of Discrete Clusters

To investigate the significance of these energy levels, P and Q, it seems feasible to utilize the basic Andrade<sup>10</sup> equation

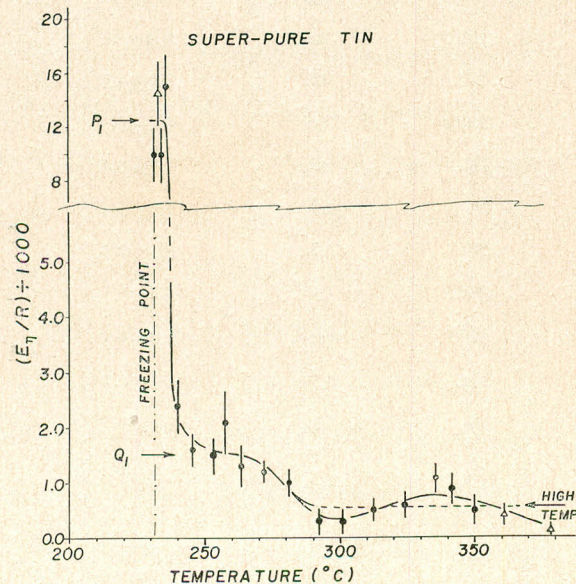
$$\eta = A \exp(E/RT) \quad (2)$$

as elaborated by Eyring,<sup>11</sup> giving

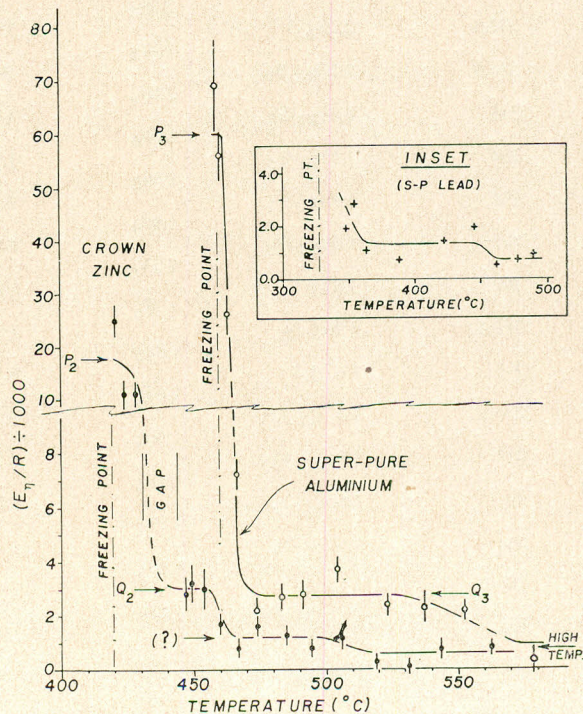
$$A = [\exp(-\Delta S/R)] \cdot h(\lambda_1/\lambda)^2 / (\lambda_1 \lambda_2 \lambda_3) \quad (3) \\ = h(\lambda_1/\lambda)^2 / [v \exp(\Delta S/R)]$$

where  $\lambda_1$ ,  $\lambda_2$ ,  $\lambda_3$  are the parameters defining the linear extension of the molecular aggregate or cluster,  $v$  is its volume,  $\Delta S$  is the entropy of activation, and  $\lambda$  is the distance between two equilibrium positions in the direction of motion, so that one may expect  $\lambda \sim \frac{1}{2}\lambda_1$  or so. Equation (3) then shows that  $A$  is inversely dependent on the volume of the cluster.

We can easily get experimental values for  $A$  from equation (2) in the form



(a)



(b)

Fig. 2.—Graphs of  $(E\eta/R)/1000$  against temperature, as calculated from Yao and Kondic's measurements, with the short vertical lines through the points indicating the estimated standard deviations, while the thin zig-zag horizontal line marks a change of scale for the ordinates: (a) super-pure tin; (b) crown zinc, solid circles; super-pure aluminium, hollow circles, with temperature scale shifted to the left by 200°C. (The hollow triangles in (a) are the means of pairs of values). *Inset to (b)*: fragmentary data for super-pure lead. In these graphs, the arrow at 'P' indicates the high constant value of  $E\eta$ , while the "Q" the intermediate region of constant  $E\eta$ , while the "High Temp." arrow marks the high-temperature values used by McLaughlin and Ubbelohde for tin and zinc.

$$\ln(1/A) = E/RT - \ln\eta, \quad (4)$$

and using the experimental values of  $\eta$  together with the deduced values of  $E/R$  shown in Figs. 2(a) and (b). The two graphs of Fig. 3 are plots of these values of  $\ln(1/A)$  against temperature for tin (left, solid circles) and zinc (right, hollow circles), both of which bring out the two regions of constant  $1/A$  at P and Q. Moreover, the actual values of  $\ln(1/A)$  appear to be nearly the same at corresponding flats of the two graphs, thus suggesting that the two metals exhibit identical types of aggregation, and so we may average the data for the two to obtain higher accuracy. The inset to Fig. 3 (right) shows a combined  $\ln(1/A)$  plot against temperature *excess* above the freezing point for tin and zinc, the four highest points (triangles) being means of successive points differing by 1°C. or less; this averaging still gives us four points in the first 9 degrees. The consistency of the data as well as the improved accuracy and resolution are apparent in the combined graph, which enables us to form some idea of the shape of the curve between the three flat regions in

addition to bringing out the constancy of  $1/A$  and (cf. equation 3) of volume 'v' over each such region thereby providing justification for continuing to use equations (2) and (3). The portion of the graph beyond 100°C. excess temperature is still unreliable (cf. the large scatter of the points) and the slight drop in  $1/A$  over this region may be no more than experimental error. Although the data for aluminium and lead are scanty and not necessarily compatible, Fig. 4 shows a tentative  $\ln(1/A)$  plot for the combined data, which shows a high-temperature value of  $4.9 \pm 0.2$  and two probable intermediate values of constant  $\ln(1/A)$ , viz. 6.6 and 5.7, the jumps occurring at nearly the same temperature excess as in Fig. 3 (inset).

In any case, Figs. 2 to 4 indicate the general occurrence of at least the two regions P and Q, of constant aggregation, where the Eyring equation should be applicable, one extending from the freezing point up for 5 deg. C. and the other from 10 deg. C. to 50 deg. C. above the freezing point. The rapid drop between the successive values of  $E_\eta$  and  $\ln(1/A)$  would probably follow the type of relations developed by McLaughlin and Ubelohde<sup>4</sup> (equations 5 and 6), as indicated by

the fact that the upper limiting values of  $E_\eta/R$  found in Fig. 2(a) and (b) above are about  $\frac{1}{2}$  of the figures estimated by these authors.

#### 4. Some Estimates of g, the No. of Atoms per Cluster at Various Temperatures

For a quantitative deduction from the Eyring equation, let us first examine the two lowest regions of constant  $\ln(1/A)$  in the inset to Fig. 3, viz. at (i)  $7.2 \pm 0.2$  from 12 to 36 degrees C. and (ii)  $4.8 \pm 0.1$  from 48 to 100 degrees C. or more above the freezing point. Since  $A = h(\lambda_1/\lambda)^2/[v \exp(\Delta S/R)]$ , we have  $v \exp(\Delta S/R) = h(\lambda_1/\lambda)^2/A$

$$\begin{aligned} &= \frac{6.62 \times 10^{-27}}{A} / (\lambda/\lambda_1)^2 \text{ cm.}^3 \\ &= \frac{6.62 \times 10^{-3}}{A} / (\lambda/\lambda_1)^2 \text{ A.U.}^3 \end{aligned} \quad (5)$$

Taking the high-temperature value  $4.8 \pm 0.1$  for  $\ln(1/A)$ , we get

$$v_{\text{high-temp}} \times \exp(\Delta S/R) = \exp(4.8) \times 6.62 \times 10^{-3} / (\lambda/\lambda_1)^2 = 0.80 / (\lambda/\lambda_1)^2 \text{ A.U.}^3, \text{ whence by taking } v_{\text{high-temp}} \text{ as the volume of a single}$$

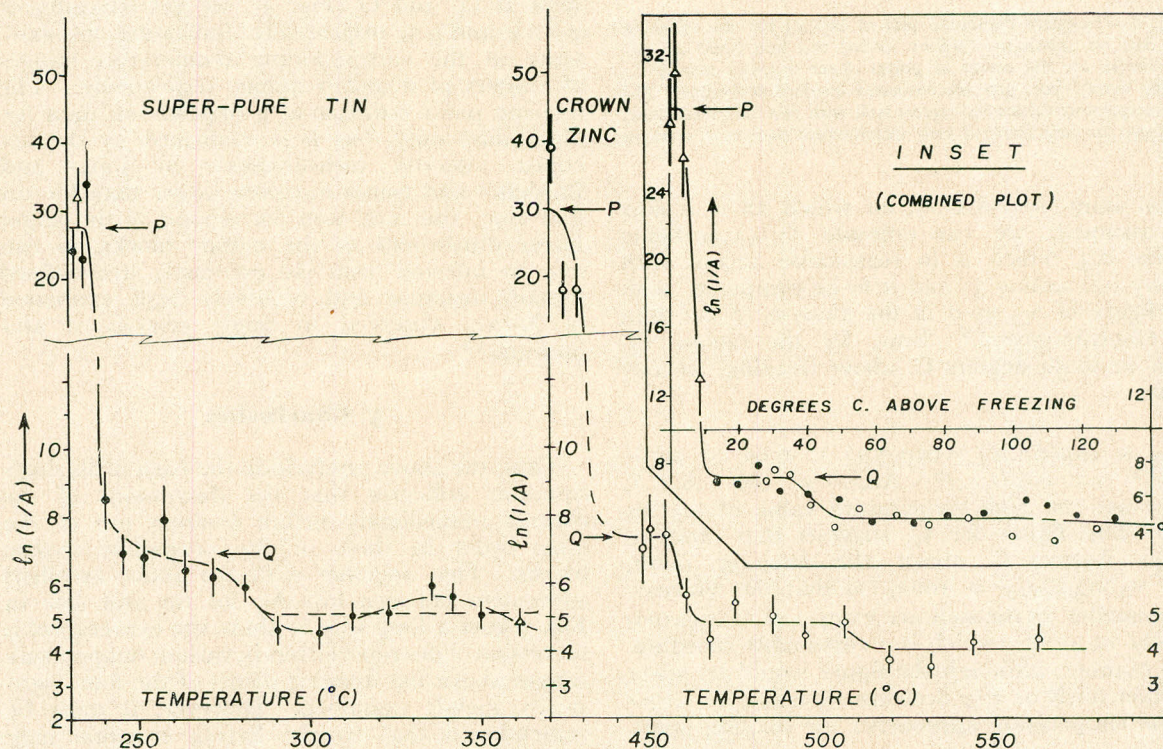


Fig. 3.—Graphs of  $\ln(1/A) \approx \text{constant} + \Delta s + \ln(\text{volume of cluster})$ , calculated from Fig. 2, showing the correspondence between (i) tin (solid circles) in left half and (ii) zinc (hollow circles) in right half; the zig-zag horizontal line indicates change of ordinate scale. The inset shows the combined plot against temperature excess above freezing point, the triangles being the means of successive points close together. P and Q mark the two regions of constant  $(1/A)$ .

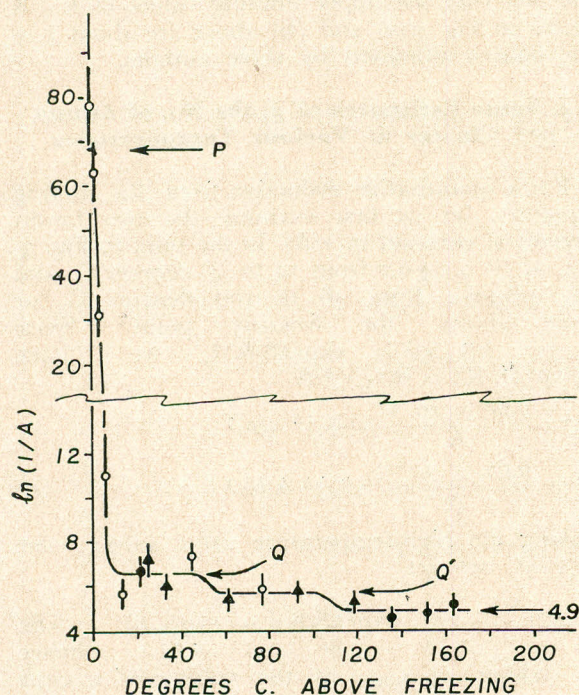


Fig. 4.—Tentative combined plot of  $\ln(1/A)$  for the relatively poor data on aluminium (hollow circles) and lead (solid circles); the triangles are the means of points closer together than  $4^\circ\text{C}$ ., and the vertical lines give the estimated standard deviations. The high temperature value of 4.9 agrees well with that for tin and zinc, and there are indications of two intermediate regions of constant  $(1/A)$ .

metal atom ( $\approx 9 \text{ A.U.}^3$ ), for which  $\Delta S \approx 0$  may be assumed, we can estimate  $(\lambda/\lambda_1)$  as being nearly 0.3, which is in reasonable accord with theory (cf. section 3) and is to be compared with the figure of 0.5 used in the analysis of the data on ethylene glycol.<sup>8</sup> Now, for the region 'Q' from 12 to 36 degrees C. above freezing, we can write

$$v_Q \times \exp(\Delta S/R) = \exp(7.2) \times 6.62 \times 10^{-3} / (\lambda/\lambda_1)^2 = 8.9 / (\lambda/\lambda_1)^2 \text{ A.U.}^3 \approx 100 \text{ A.U.}^3,$$

if we use the high-temperature value of 0.3 for  $\lambda/\lambda_1$ . This figure for  $v_Q$  suggests that from 12 to 36 degrees C. above the freezing point,  $g = v_Q/v_{\text{high-temp}} \approx 100/9$ , so that the 'clusters' or 'miscelles' in the melt are composed of approximately 12 atoms, which is a reasonable coordination number, although the figure would be lower if either  $\Delta S/R$  or  $\lambda/\lambda_1$  becomes significantly larger as the temperature approaches the freezing point.

When this mode of analysis is extended to the narrow  $5^\circ$  region 'P' of highest  $(1/A)$  just above the freezing point, we get

$$v_P \times \exp(\Delta S/R) = \exp(29) \times 6.62 \times 10^{-3} / (\lambda/\lambda_1)^2 = 26 \times 10^9 / (\lambda/\lambda_1)^2 \text{ A.U.}^3$$

which on neglecting  $\Delta S/R$  yields a volume corresponding to the presence of as many as  $10^{10}$  atoms in a cluster. If we estimate  $\Delta S$  near freezing to be of the order of  $2L/T$ , i.e.  $\sim 4R$ , then  $v$  is diminished 50-fold, making the linear dimensions of the cluster about  $2 \times 10^3 \text{ \AA}$ , i.e. 0.2 microns.\* This may seem large, but because these are to be thought of as potentially crystalline clusters it is perhaps not excessive, and is in fact of the order of the probable dimensions of the "mosaic" blocks ( $1-0.1 \mu$ ) in crystals.<sup>12, 13</sup> For further comparison, some (unpublished) calculations (Buckle, quoted in reference 4) would give an estimate of 0.03 microns for nuclei giving spontaneous crystallization about  $100^\circ\text{C}$ . below the freezing point of tin. Of course, McLaughlin and Ubbelohde's estimate of the pre-freezing value of  $g$  lies between our estimates corresponding to the two flats at P and Q.

For aluminium (and lead), the high temperature value of  $\ln(1/A)$  ( $4.9 \pm 0.2$ ) is very close to that for tin and zinc, so that the same value of  $\lambda/\lambda_1$  ( $\approx 0.3$ ) is obtained. From the two intermediate steps at Q' and Q (Fig. 4), we get estimates of  $g = 2.2$  and 5.5, respectively, indicating the existence in the corresponding temperature ranges of clusters of 2 and 6 atoms, respectively. The freezing point estimate of  $g$  depends on data for aluminium only, but it is confirmed by the accurate viscosity measurements of Jones and Bartlett,<sup>3</sup> and comes out even larger than for tin and zinc; this may well correspond to the larger linear dimensions of the mosaic blocks, as can also be inferred from the extremely well-defined mosaic structure and relatively high extinction of X-rays observed in single crystals of aluminium.<sup>12</sup>

## 5. Conclusion

Thus, the above analysis on the basis of Eyring's equation indicates that the dimensions of the clusters immediately before freezing are of the same order as those of the crystalline mosaic blocks. This, together with the above excellent agreement between  $\ln(1/A)$  for tin and zinc in Fig. 3 goes a long way to show the existence of a succession of discrete clusters in various temperature ranges above the freezing points of the four high-purity metals examined. However, it must be remembered that (i) the Eyring equation may need incorporation of McLaughlin and Ub-

\*For an elongated cluster with  $\lambda/\lambda'$  increased ten times, the estimated volume would decrease 100 fold, while the length would remain the same as for an equidimensional cluster.

belohde's ideas of suspensions of clusters to give a complete picture of the viscous interactions close to the freezing point, and (ii) the measurements of viscosity very close to the freezing point are liable to serious disturbance by such factors as temperature gradients and oxide formation. For a more complete analysis of the nature of the structure within the clusters and the kinetics of their interactions, there is a clear need for more exhaustive and accurate measurements in the pre-freezing region, possibly by a differential technique like that described in section 1, both for metals and pure organic compounds.

#### References

1. M. M. Qurashi, *J. Phys. Chem.*, **67**, 955 (1963).
2. T. P. Yao and V. Kondic, *J. Inst. Metals*, **81**, 17 (1952-53).
3. W. R. D. Jones and W. L. Bartlett, *J. Inst. Metals*, **81**, 145 (1952-53).
4. E. McLaughlin and A. R. Ubbelohde, *Trans. Faraday Soc.*, **56**, 988 (1960).
5. M. M. Qurashi and A. K. M. Ahsanullah, *Brit. J. Appl. Phys.*, **12**, 65 (1961).
6. A. Rauf and M. M. Qurashi, *Pakistan J. Sci. Ind. Research*, **2**, 30 (1959).
7. A. K. M. Ahsanullah, S. R. Ali and M. M. Qurashi, *Pakistan J. Sci. Ind. Research*, **5**, 110 (1962).
8. A. K. M. Ahsanullah and M. M. Qurashi, *Brit. J. Appl. Phys.*, **13**, 334 (1962).
9. A. M. Chowdhry, H. Ahmad and M. M. Qurashi, *Pakistan J. Sci. Ind. Research*, **3**, 101 (1960).
10. A. N. da C. Andrade, *Phil. Mag.*, **17**, 698 (1934).
11. S. Glasstone, K. J. Laidler and H. Eyring, *The Theory of Rate Processes* (McGraw-Hill, New York, 1941), pp. 480-516.
12. R. W. James, *The Optical Principles of the Diffraction of X-rays* (G. Bell & Sons, London, 1948), pp. 268-286.
13. A. H. Compton and S. K. Allison, *X-rays in Theory and Experiment* (Van Nostrand Co., New York, 1935), p. 400 *et seq.*